Eur Radiol
DOI 10.1007/s00330-012-2440-3

CHEST

Analysis of the impact of digital tomosynthesis on the radiological investigation of patients with suspected pulmonary lesions on chest radiography

Emilio Quaia · Elisa Baratella · Stefano Cernic · Arianna Lorusso · Federica Casagrande · Vincenzo Cioffi · Maria Assunta Cova

Received: 1 November 2011 / Revised: 5 February 2012 / Accepted: 10 February 2012

Abstract
Objective To assess the impact of digital tomosynthesis (DTS) on the radiological investigation of patients with suspected pulmonary lesions on chest radiography (CXR).
Methods Three hundred thirty-nine patients (200 male; age, 71.19±11.9 years) with suspected pulmonary lesion(s) on CXR underwent DTS. Two readers prospectively analysed CXR and DTS images, and recorded their diagnostic confidence: 1 or 2=definite or probable benign lesion or pseudolesion deserving no further diagnostic workup; 3=indeterminate; 4 or 5=probable or definite pulmonary lesion deserving further diagnostic workup by computed tomography (CT). Imaging follow-up by CT (n=76 patients), CXR (n=256) or histology (n=7) was the reference standard.
Results DTS resolved doubtful CXR findings in 256/339 (76 %) patients, while 83/339 (24 %) patients proceeded to CT. The mean interpretation time for DTS (mean±SD, 220±40 s) was higher (P<0.05; Wilcoxon test) than for CXR (110±30 s), but lower than CT (600±150 s). Mean effective dose was 0.06 mSv (range 0.03–0.1 mSv) for CXR, 0.107 mSv (range 0.094–0.12 mSv) for DTS, and 3 mSv (range 2–4 mSv) for CT.
Conclusions DTS avoided the need for CT in about three-quarters of patients with a slight increase in the interpretation time and effective dose compared to CXR.
Key Points
• *Digital tomosynthesis (DTS) improves the diagnostic confidence of chest radiography (CXR)*
• *DTS reduces the need for CT for a suspected pulmonary lesion*
• *DTS only imparts a radiation dose of around two CXRs*
• *DTS takes longer to interpret than conventional chest radiography*

Keywords Radiography · CT · Tomosynthesis · Lung · Chest

Abbreviations

CXR	Chest radiography
DTS	Digital tomosynthesis
CT	Computed tomography

Introduction

The detection and characterisation of pulmonary lesions, and particularly of pulmonary nodules, are challenging tasks on chest radiography (CXR) because of their frequently small size and poor conspicuity against surrounding anatomical structures. Pulmonary lesions are often visible only retrospectively when reviewing previous radiographic images of patients with known nodules [1], and computer-aided detection systems have been advocated to improve the diagnostic accuracy [2]. Frequently, the radiologist reporting CXR identifies doubtful or equivocal findings that could be due to pulmonary or extrapulmonary lesions or even pseudolesions due to composite areas of increased opacity.

Even though oblique radiographic views or chest fluoroscopy is still frequently employed, computed tomography (CT) is the gold standard for imaging pulmonary lesions, in particular pulmonary nodules [3, 4]. However, it is relatively expensive, delivers a considerable radiation dose, and may

E. Quaia (✉) · E. Baratella · S. Cernic · A. Lorusso · F. Casagrande · V. Cioffi · M. A. Cova
Department of Radiology, Cattinara Hospital, University of Trieste (Italy), Strada di Fiume 447, 34149 Trieste, Italy
e-mail: equaia@yahoo.com

Published online: 27 April 2012

delay diagnosis because of CT unit work overload. Therefore, CXR remains the initial examination for most lung lesions, with CT being normally used to confirm the diagnosis in doubtful cases. As such, CT is frequently performed in patients without any pulmonary lesions or with pulmonary lesions that appear clearly benign or extrapulmonary after CT [1, 3, 4].

Digital tomosynthesis (DTS) [5, 6] is a tomographic technique like CT, but delivers a lower radiation dose [5–8]. DTS is easily implemented in conjunction with CXR as it employs the same X-ray equipment. Unlike conventional tomography, DTS is not limited to reconstruction of a single plane, but can generate an arbitrary number of slice planes throughout the entire volume of the patient. Reconstruction of the image planes is performed from a set of projection data acquired over a limited angle range of a single X-ray tube. A series of projection radiographs are acquired during the X-ray tube movement, and, due to the parallax effect, the anatomy at different depths in the patient can be mapped by the projections. These projections are then shifted and added to bring objects in a given plane into focus. By varying the amount of shift, planar images at different depths can be reconstructed [7–9], and objects outside of the focus plane are rendered with a varying amount of blur.

Previous studies have shown that DTS vs CXR improved sensitivity in the detection of CT-proven lung nodules [7–10], and that DTS provides high diagnostic accuracy and confidence in confirming or ruling out those pulmonary lesions suspected on CXR by improving pulmonary lesion conspicuity [11, 12]. According to these results DTS could be considered a problem-solving technique in those patients with suspected pulmonary lesions on CXR and could be used in the place of CT in this particular clinical setting. However, no previous study has evaluated the actual impact provided by DTS both on the CT utilisation rate and patient diagnostic workflow.

The aim of this study was to assess the impact of DTS on the radiological investigation of patients with suspected pulmonary lesions on CXR.

Methods and materials

Patients

This was a single-centre prospective study approved by the ethics committee of the Cattinara Hospital, University of Trieste (Italy), and informed consent was obtained from all patients after the nature of the procedure was fully explained. From June 2007 to March 2011, all patients who revealed suspected pulmonary lesion(s) appearing as areas of increased opacity or pulmonary nodules [13] on CXR underwent DTS. CXR was obtained in the upright postero-anterior and left lateral views, and the preliminary CXR interpretation was performed by two board-registered diagnostic radiologists (E.B. and V.C.) affiliated to our department and experience in thoracic imaging of 10 and 25 years, respectively. Suspected pulmonary lesions were those that could not reliably be considered present or located within the lung, based only on CXR interpretation.

Inclusion criteria were: DTS performed within 15 days from CXR and absence of respiratory artefacts on DTS images preventing correct image assessment. Of the 368 patients who were deemed initially eligible for the study (Fig. 1), 29 were

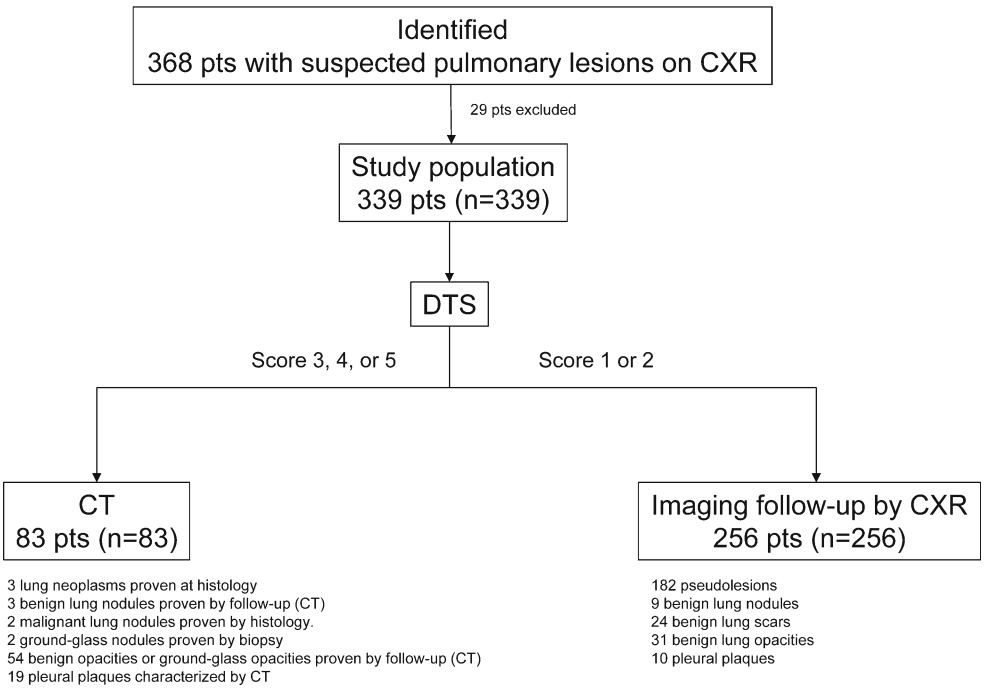

Fig. 1 Flow diagram of the patient study group. Numbers between brackets are lesion number. CXR = chest radiography; DTS = digital tomosynthesis

excluded for the following reasons: (1) the patients had previous chest surgery (n=2); (2) the patients had subdiagnostic DTS images because of inability to keep the upright position or suspend respiration (n=2); loss of patients' information or incomplete patient follow-up (n=25). The 339 patients (age 71.19±11.9 years) who met the inclusion criteria included 200 men (mean age 70.4 years±10.7; median age 71 years; age range 23–94 years) and 139 women (mean age 72.6 years± 12.4; median age 73 years; age range 34–97 years), and these patients were considered in the present study (Table 1).

Digital tomosynthesis

The radiographical system (Definium 8000; GE Healthcare, Chalfont St Giles, UK) consisted of an X-ray tube (focal spot size 0.6 mm), a wall stand, a stationary antiscatter grid (70 lines per cm; ratio 13:1), and a cesium iodide-amorphous silicon (CsI/a-Si) indirect flat-panel detector (41×41 cm^2; 200×200 mm^2 pixel size) with CsI/a-Si in a columnar structure. X-rays are converted to light in a layer of thallium-doped CsI, then the light is converted to electrical signals by a-Si photodiodes, and the signal is multiplexed to the readout electronics by thin-film transistors (TFT) consisting of a-Si deposited on a glass substrate. The signal is digitised with 14-bit resolution (16 384 grey levels) by external electronics.

We employed the VolumeRAD option of the digital X-ray system, which acquires a series of very low-dose projection images during a single linear sweep of the X-ray tube over an angle of 30° with a stationary detector. A scout image is first obtained to check the patient position. If the scout image is satisfactory, the system calculates the appropriate low-dose exposure (mAs) for DTS. Acquisition data were: voltage 120 kVp; detector entrance dose 0.5 μGy; nominal focal spot 0.6 mm; additional copper filtration 0.1 mm; breath-hold acquisition time 11 s; 60 low-dose projection images were acquired at regular angular intervals during the tube sweep. These data were then reconstructed with a filtered backprojection algorithm to generate a set of images at a 5-mm plane interval and a default number of slices depending on patient size (41, 53, or 61 slices for a body mass index <18.5, from 18.5 to 25, or >25, respectively). All projection images were used for the reconstruction of each plane.

Table 1 Radiographic pattern of lesions

Diagnoses	n	Mean size (cm) ± SD	Size range (cm)
Pulmonary opacities	8	2.5±0.3	2–3
Primary lung neoplasms§	3	2.5±0.7	2–3
Noncalcified Pulmonary scars*	8	1.1±0.3	0.5 - 1.5
Ground-glass opacities/nodules#	47	2.5±0.4	2–3
Non-calcified solid nodulesΔ	14	1.1±0.3	0.5 – 1.5
Calcified solid nodules/scars	48	1.1±0.3	0.5 – 1.5
Pleural plaques	29	2.4±0.6	1–3
Pulmonary pseudolesions‡	182	–	–
Total number	339	2.3±1.1	0.5 - 4

Note: Radiographic patterns of lesions included in the present study

§Lung adenocarcinomas proven by histology and corresponding to a focal mass opacity with irregular or spiculated margins, and/or scissure or pleural or vessel infiltration on CT

*Areas of focal opacity or parenchymal bands with architectural distortion due to fibrosis with or without gross calcifications

#Ground-glass pattern as observed on CT, including two indolent lung adenocarcinomas proven by biopsy

ΔIncludes two lung adenocarcinomas proven by histology

‡Includes composite areas of increased opacity resulting from overlap of vascular and bone structures of the chest (n=137 patients), consolidated rib fractures or osteophytes of the costovertebral articulation (n=36), vascular kinkings (n=4), prominent cardiac auricular or epicardial adipose tissue (n=3), and accessory fissures (n=2)

Image analysis

Visual analysis of CXR and DTS images of each patient was carried out within 7 days from DTS by the same two radiologists who performed the initial CXR assessment. Image analysis was performed for patient care, and the CXR and DTS images of each patient were examined consecutively in the same reading session according to the routine diagnostic workflow. During the image analysis both readers worked independently and were aware of patient identification and clinical history, but were blinded to biopsy results and other imaging findings. Readers were allowed to use processing tools such as windowing, image contrast, adjustment, or magnification, and to scroll the DTS images. All readings were performed on a picture archiving and communications system (PACS)–integrated workstation (19-inch TFT display, resolution 2,560×1,600 pixels) at a central location. The first one or two cases were used for training to familiarise the radiologist with the process.

Readers were asked to re-identify those findings on the CXR images that led each patient to undergo DTS. For those patients (n=19) with more than one suspected pulmonary lesion on CXR, the largest and most conspicuous finding was consensually considered as the marker lesion. Then, both readers were asked to confirm or exclude the same finding on DTS images, and to express diagnostic confidence about lesion nature and pulmonary or extrapulmonary location according to the scoring system reported in Table 2.

Radiologists were timed by the principal investigator responsible for the study (E.Q.) while they were interpreting CXR and DTS. Radiologists were also timed while they

Table 2 Confidence scoring system

Confidence score	Reader finding
1 or 2	Definite or probable
	(1) Benign pulmonary* or extrapulmonary lesion§
	(2) Pulmonary pseudolesion#
3	Indeterminate⌂
4 or 5	Probable or definite pulmonary lesionΔ

Note: Diagnostic confidence scoring system

*Centrally calcified pulmonary lesions or pulmonary lesions with gross calcifications or calcified fibrotic scars with pulmonary architectural distortion

§Lesions not contained in the limits of lung parenchyma (e.g. pleura or thoracic wall) with or without calcifications

#Opacity not due to a true pulmonary or extrapulmonary lesions, but to normal anatomical structures including composite areas of increased opacity due to overlap of vascular and bone structures of the thoracic wall, vascular kinking, anatomic variant, rib fracture, bone island, or osteophytes

⌂Readers failed to classify confidently the presence of a lesion, or whether a lesion was pulmonary or extrapulmonary or was a pseudolesion

ΔA solid pulmonary lesion, a parenchymal or ground-glass opacity, or a solid or subsolid ground-glass pulmonary nodule

were interpreting the CT images for those patients who underwent chest CT after DTS. Reader interpretation times were measured from the start of image evaluation and excluded the time necessary for the written report. Each case was read only once. A time-stamp macro (Excel; Microsoft, Redmond, WA, USA) was used by the primary investigator to record the start time of the reading process. Once the case was interpreted, the principal investigator recorded the final time. This process was repeated for each case.

Patient clinical management

The patient diagnostic workup was planned based on the readers' confidence score for DTS images (Fig. 1). Discrepant interpretations determining a potential change in the patient management were resolved by consensus through the involvement of an additional reader with similar experience in thoracic imaging. When DTS images were scored as 1 or 2, which is the identification of definite or probable benign pulmonary or extrapulmonary lesions or pulmonary pseudolesions, the imaging follow-up was perfomed by CXR, which was repeated after a mean time of 6 months (time range 3–8 months) from DTS. When DTS images were scored as 3, 4, or 5, which defined indeterminate or probable or definite pulmonary lesions, patients underwent CT within 1 week.

Reference standards

Figure 1 reports the patient diagnostic flowchart including the reference standards. When DTS images were scored as 1 or 2, the imaging follow-up was a repeat CXR (n=256 patients; Fig. 1) a mean of 6 months (range 3–8 months) after DTS. Considering the imaging findings obtained by DTS, the imaging follow-up was stopped when CXR did not confirm any pulmonary lesion or confirmed the presence of overt benign pulmonary or extrapulmonary lesions.

When DTS images were scored as 3, 4, or 5, patients underwent CT within 1 week (n=76 patients). All lesions were considered benign if they contained fat or were calcified or subsequently disappeared during imaging follow-up, or decreased or remained unequivocally stable in size during serial examinations.

Those lesions appearing as ground-glass opacities on CT and that did not disappear during CT follow-up underwent CT-guided biopsies (n=2 patients). All lesions presenting overt malignant features at CT (irregular or spiculated margins, pleural or vascular infiltrations) underwent surgical resection (n=5 patients), while the remaining lesions were characterised by CT follow-up performed at least 6 months apart for a minimal period of 2 years.

CT examination

CT of the chest was performed with 64-row multi-detector CT (Aquilion, Toshiba, Tokyo, Japan). Patients were instructed to hold their breath with tidal inspiration during scanning. CT examinations consisted of an unenhanced CT data acquisition followed by a vascular phase acquired 40 s after the intravenous bolus injection of iodinated contrast material (Iomeron 350, Bracco, Milan, Italy; 350 mg I/ml, 3 ml/s at 2 ml/kg followed by 50 ml of saline flush) administered with a dual-syringe power injector (Stellant CT injector, Medrad, Indianola, PA, USA) via a 20-gauge catheter inserted into an antecubital vein.

CT images at standard lung window settings (window level of −600 HU and window width of 2000 HU) were analysed immediately after image acquisition by a consensus of two senior radiologists with 8–15 years of experience in chest imaging who were not involved in the visual interpretation of CXR or DTS images and were affiliated to the radiology department where the study was performed. Readers were free to scroll CT images and to employ coronal or sagittal reformations to measure the largest diameter of each thoracic lesion in each plane.

The CT utilisation rate, defined as the number of CTs performed following the CXR divided by the number of CXR, was calculated before (control period) and after DTS implementation. The observational time before and after DTS implementation was divided into: (1) the control

Table 3 Diagnostic performance and confidence

		CXR					DTS				
Reader 1	Sensitivity (%)	9 (7/80)					91 (72/80)				
	Specificity (%)	9 (25/259)					92 (240/259)				
	PPV (%)	2 (7/241)					79 (72/91)				
	NPV (%)	25 (25/98)					96 (240/248)				
	Accuracy (%)	9 (32/339)					92 (312/339)				
	Diagnostic confidence:										
		Number	TP	TN	FP	FN	Number	TP	TN	FP	FN
	Score 1	1	/	1	/	/	234	/	234	/	/
	Score 2	35	/	24	/	11	8	/	6	/	2
	Score 3	276§	/	/	214	62	9*	/	/	3	6
	Score 4	23	7	/	16	/	42	29	/	13	/
	Score 5	4	0	/	4	/	46	43	/	3	/
	(AUC) (95 % CI)	0.507 (0.434–0.580)					0.979 (0.975–1)				
Reader 2	Sensitivity (%)	5 (4/80)					92 (74/80)				
	Specificity (%)	16 (43/259)					92 (240/259)				
	PPV (%)	2 (4/220)					79 (74/93)				
	NPV (%)	36 (43/119)					97 (240/246)				
	Accuracy (%)	13 (47/339)					93 (314/339)				
	Diagnostic confidence:										
		Number	TP	TN	FP	FN	Number	TP	TN	FP	FN
	Score 1	2	/	1	/	1	233	/	232	/	1
	Score 2	45	/	42	/	3	9	/	8	/	1
	Score 3	281§	/	/	209	72	9*	/	/	5	4
	Score 4	10	4	/	6	/	27	18	/	9	/
	Score 5	1	0	/	1	/	61	56	/	5	/
	(AUC) (95 % CI)	0.565 (0.491–0.639)					0.984 (0.965–1)				

Note: CXR, chest radiography; DTS, digital tomosynthesis; TP, true positive (lesion correctly assessed as a non-calcified pulmonary lesion (confidence score 4 or 5) or a lesion appearing as a parenchymal or ground-glass opacity, or a solid or subsolid ground-glass pulmonary nodule); TN, true negative (benign pulmonary-centrally calcified lesion or lesion with gross calcifications or calcified fibrotic scars with pulmonary architectural distortion-or extrapulmonary lesion or as a pulmonary pseudolesion (confidence levels 1, 2); NPV, negative predictive value; PPV, positive predictive value. AUC, area under the receiver-operating characteristic curve; CI, confidence interval

Visual prospective analysis in the pulmonary lesion diagnosis

The confidence scoring system is reported in Table 2

All differences between chest radiography and digital tomosynthesis were statistically significant ($P<0.05$)

§Including 62 (reader 1) or 72 (reader 2) solid pulmonary lesions and 214 (reader 1) or 209 (reader 2) pseudolesions, extrapulmonary lesions, or overt benign pulmonary lesions

* Including 6 (reader 1) or 4 (reader 2) solid pulmonary lesions, and 3 (reader 1) or 5 (reader 2) pseudolesions, extrapulmonary lesions, or overt benign pulmonary lesions

period defined as the 12-month period (from 1 June 2006 to 31 May 2007) preceding DTS implementation in our radiology department; (2) the 12-month period following DTS implementation (from 1 June 2007 to 31 May 2008) when the radiology department was tuning up the diagnostic workflow; (3) the following period (from 1 June 2008 to 31 May 2011) corresponding to established DTS use in the routine clinical diagnostic workup, which was divided into the second (from 1 June 2008 to 31 May 2009), third (from 1 June 2009 to 31 May 2010), and fourth (from 1 June 2010 to 31 May 2011) year after DTS implementation.

Estimation of effective dose

The X-ray system employs a dose indicator, which calculates the dose-area product (DAP) from the exposure parameters. The DAP indicator was calibrated every 6 months. The DAP was recorded (in milligrays per cm^2) together with the examination procedure time.

Data were analysed by a PC-based X-ray Monte Carlo program, PCXMC 2.0 (Radiation and Nuclear Safety Agency, Helsinki, Finland) [14]. This software allows Monte Carlo simulation for calculation of patient dose in X-ray examinations. The mathematical phantom used in PCXMC

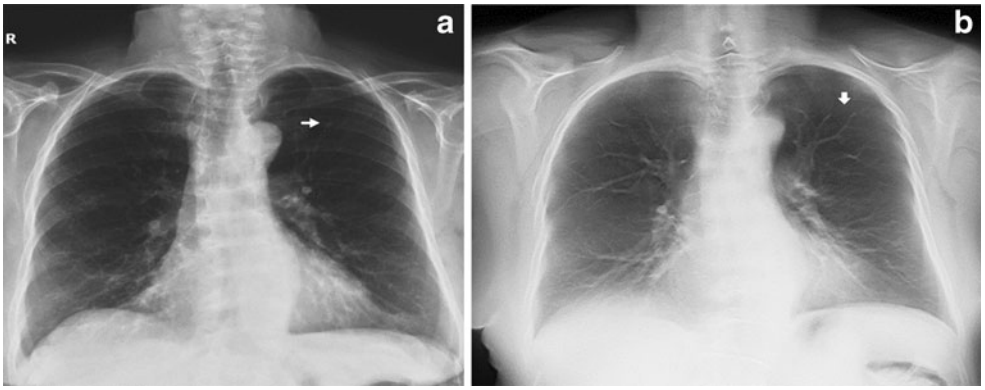

Fig. 2 A 60-year-old man with a vascular kinking in the left chest cavity that was incorrectly identified as a pulmonary lesion upon chest radiography. **a** Posteroanterior chest radiography in the upright position shows one suspected pulmonary nodule in the left lung (*arrow*). **b** Digital tomosynthesis image clarifies that the same opacity was due to vascular kinking (*arrow*), and both readers provided a confidence score of 1

2.0 for the adult phantom is based on the model specified by Cristy and Eckerman [15]. We employed the method previously described in [16] to calculate the effective dose for the postero-anterior and left lateral projections of CXR and for each DTS projection view. For the postero-anterior and left lateral projection views, 10^7 primary x-ray photon histories were simulated per energy bin. For each of the DTS projections, 10^6 primary x-ray photon histories were simulated per energy bin for a total of 6×10^7 histories per energy bin for the complete DTS data set. This resulted in less than 0.1 % statistical error in the simulation of the effective dose values for the PA, lateral, and each DTS projection view [16]. The x-ray beam size was adjusted according to the projection acquisition [16].

The CT effective dose estimate was determined by using dose length product (DLP) measurements and appropriate normalised coefficients found in the European guidelines [17] for chest CT (0.017 mSv × mGy^{-1} × cm^{-1}).

Statistical analysis

Statistical analysis was performed with a computer software package (Analyse-it, version 1.63, Analyse-it-software, Leeds, UK). A per-patient analysis was performed with the marker lesion considered for the calculation of sensitivity, specificity, positive and negative predictive values, and overall diagnostic accuracy. True positive was a lesion correctly assessed as a non-calcified pulmonary lesion (confidence score 4 or 5) or a lesion appearing as a parenchymal or ground-glass opacity, or a solid or subsolid ground-glass pulmonary nodule; false negative a pulmonary lesion incorrectly assessed as a benign pulmonary or extrapulmonary lesion or as a pulmonary pseudolesion (confidence score of 1 or 2) or assessed as indeterminate (confidence score 3); true negative a lesion correctly assessed as a benign pulmonary-centrally calcified lesion or lesion with gross calcifications or calcified fibrotic scars with pulmonary architectural distortion—or an extrapulmonary lesion or as a pulmonary pseudolesion (confidence levels 1, 2);

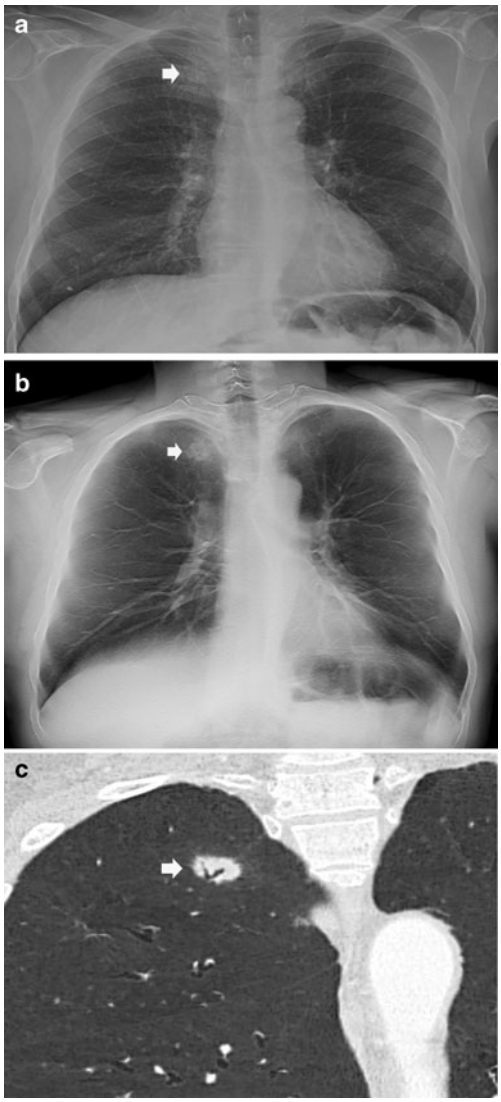

Fig. 3 A 65-year-old man with a peripheral pulmonary ground-glass pulmonary nodule. **a** Posteroanterior chest radiography in the upright position shows one suspected pulmonary opacity of the apex of the right lung (arrow) behind the overlying anterior arch of the first right rib. **b** Digital tomosynthesis planes show a ground-glass pulmonary nodule (arrow) with evidence of intralesional air bronchogram. **c** CT image (lung window, coronal reformation) confirms the same opacity with a similar feature as shown by digital tomosynthesis

Fig. 4 A 55-year-old man with a solid pulmonary nodule. **a** Posteroanterior chest radiography in the upright position shows one linear opacity on the periphery of the left lung (arrow). **b** Digital tomosynthesis planes show one solid nodular opacity (arrow) with peripheral spiculations that revealed a pulmonary location (both readers provided a confidence score of 5). **c** CT image (lung window, transverse plane) confirms the same nodule with a similar extension as shown by digital tomosynthesis

false positive a benign pulmonary or extrapulmonary lesion, or a pulmonary pseudolesion incorrectly assessed as a pulmonary lesion deserving further evaluation by CT (confidence levels 4 or 5) or assessed as indeterminate (confidence score 3).

To assess the improvement in observers' performance in correctly diagnosing pulmonary lesions, McNemar's test [18] was employed for sensitivity, specificity, and positive and negative predictive values, and the chi-square test with Yates correction [19] for accuracy. The improvement in diagnostic confidence was assessed by receiver-operating characteristic (ROC) curve analysis by plotting the sensitivity (true-positive fraction) against 1-specificity (false-positive fraction). The area under each ROC curve was calculated by using a non-parametric method [19], and the method proposed by Hanley and McNeil [20] was employed to compare the areas under each ROC curve.

The weighted *k* statistic was calculated to assess intra- and inter-group observer agreement [21]. Agreement was graded as poor (k value <0.20), fair (≥0.20 and <0.40), moderate (≥0.40 and <0.60), good (≥0.60 and <0.80), and very good (≥0.8 up to 1).

The difference between the CT utilisation rate during the control period and treatment periods and the reader interpretation time for CXR and DTS were compared by Wilcoxon's signed rank test. For all statistical tests, a *P* value <0.05 was considered to indicate a statistically significant difference.

Results

Final diagnoses included 128 pulmonary and 29 pleural lesions in 157/339 patients, and pulmonary pseudolesions in the remaining 182/339 patients (Table 1). Table 3 reports the different values of diagnostic performance and confidence for CXR and DTS. CXR vs. DTS differed in sensitivity, specificity, positive and negative predictive values, and overall diagnostic accuracy and area under the ROC curve for both readers. Inter-reader agreement improved from moderate with CXR (k values=0.40) to very good with DTS (k value=0.89).

According to the final clinical diagnosis, DTS correctly classified 312 (reader 1) or 314 (reader 2) lesions (Figs. 2, 3,

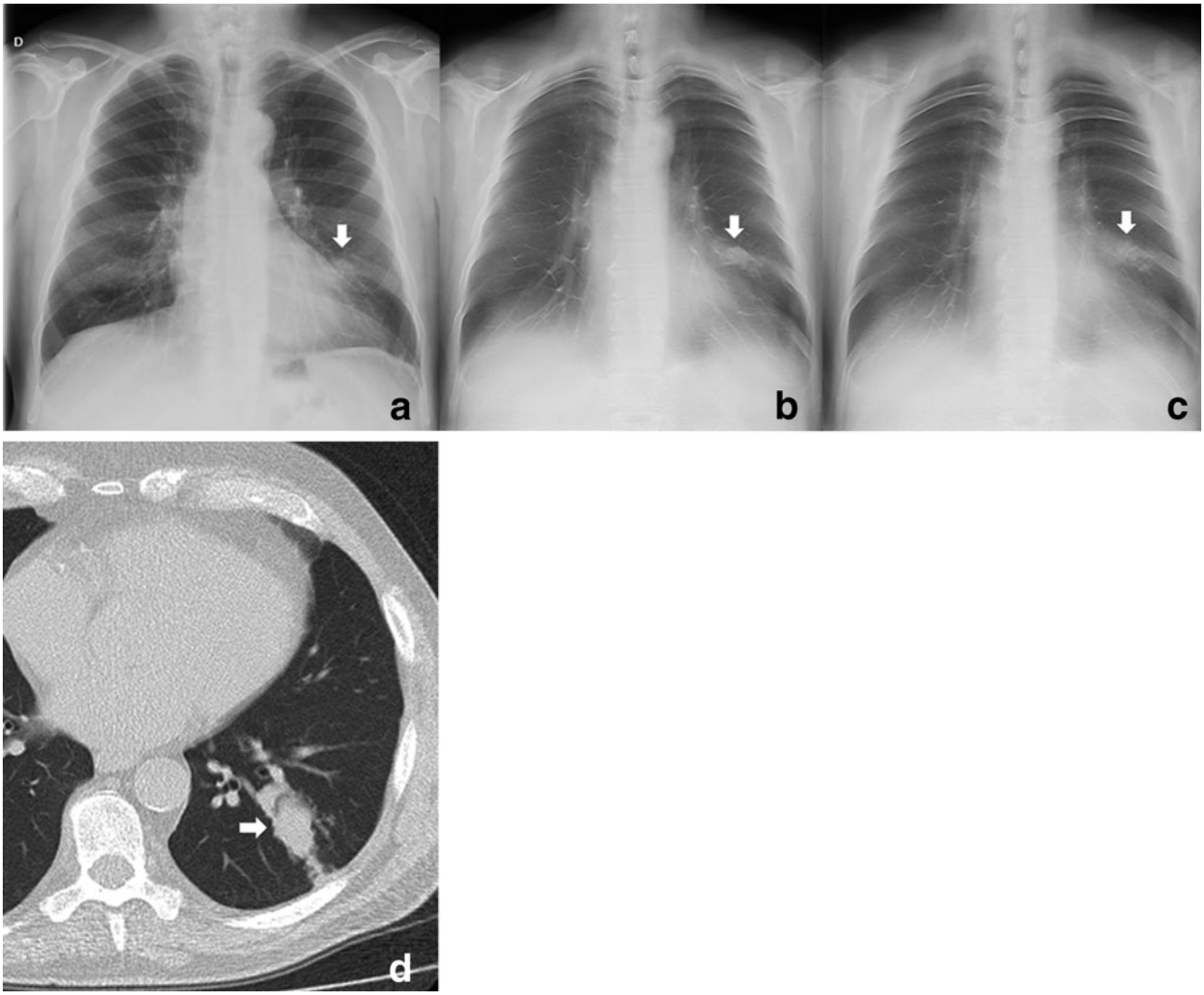

Fig. 5 A 75-year-old man with a peripheral pulmonary opacity. **a** Posteroanterior chest radiography in the upright position shows suspected opacity on the left lung (arrow) near the cardiac left profile. **b**, **c** Digital tomosynthesis planes confirm the opacity (arrow) even though it was classified as indeterminate (score 3) by both readers who were not able to classify the lesion as pulmonary or extrapulmonary. **d** CT image (lung window, transverse plane) located the same opacity in the left lung (arrow)

and 4), while in 19 (both readers) non-calcified pleural plaques and in 8 (reader 1) or 6 (reader 2) pulmonary lesions (appearing as nodules or opacities both on CXR and DTS) the readers were not able to classify confidently whether a lesion was pulmonary or extrapulmonary. Those were subpleural lesions or lesions located in the anterior or posterior region of the lung parenchyma in the proximity of the thoracic wall (Fig. 5).

The mean interpretation time for DTS (mean ± SD, 200± 40 s) was longer ($P<0.05$) than for CXR (120±30 s) but shorter than CT (600±150 s).

Table 4 reports the CT utilisation rate according to the different observational periods. The number of CTs performed for suspected lesions on CXR during the different observational periods is shown in Fig. 6. After DTS implementation 83/339 (24 %) patients underwent chest CT, while in the remaining 256/339 patients (76 %) CXR doubtful findings were resolved by DTS ($P<0.05$).

Mean effective dose was 0.06 mSv (range 0.03–0.1 mSv) for CXR, 0.107 mSv (range 0.094–0.12 mSv) for DTS, and 3 mSv (range 2–4 mSv) for CT depending on the tube current.

Discussion

Numerous methods have been proposed to address perceptual limitations in CXR including dual-energy chest radiography, bone subtraction, and computer-aided diagnosis (CAD), and these methods have experienced varying levels of success. One of the most recent and promising technological advancements

Table 4 CT utilisation rate after suspicious findings on chest radiography

	CT utilisation rate§
Control period	0.33 (271 / 811)#
After digital tomosynthesis implementation	0.24 (83 / 337)
First year	0.3 (39 / 130)
Second year	0.26 (20 / 75)
Third year	0.17 (14 / 81)
Fourth year	0.19 (10 / 51)

Note: CT utilisation rate after suspicious findings on chest radiography according to the different observational periods. Patient numbers are in parentheses

#Digital tomosynthesis not yet implemented

§CTs performed following chest radiography divided by the number of chest radiographs in which a pulmonary lesion(s) was suspected

Control period: 1 June 2006-31 May 2007. First year after digital tomosynthesis implementation: 1 June 2007-31 May 2008. Second year: 1 June 2008-31 May 2009. Third year: 1 June 2009-31 May 2010. Fourth year: 1 June 2010-31 May 2011

for improving the diagnosis of subtle lesions in the chest is DTS [7–12]. In comparison to CXR, DTS produces superior images for identifying the intra- or extrapulmonary lesions previously suspected based on initial CXR interpretation. The major advantages of DTS over conventional CXR are the removal of overlying anatomical structures, the enhancement of local tissue separation, and availability of depth information of the structure of interest [5–7].

In this study DTS was confirmed to be decisive to confirm or rule out pulmonary lesions and to differentiate true pulmonary opacities from those due to pleural or thoracic wall lesions or pulmonary pseudo-lesions [21] with a clear improvement in diagnostic accuracy, confidence and inter-reader agreement in comparison to CXR and with a modest increase in the radiation dose and interpretation time. In our series CXR revealed low sensitivity and specificity because most of these lesions were scored as suspected or indeterminate on CXR and thereby considered to be false-negative findings. This presents a strong clinical impact, since up to 20 % of suspected nodules on CXR can be entities mimicking a solitary nodule [22]. In our series, we found an even higher percentage of pulmonary pseudolesions (53 %) leading the patients to DTS. According to these results, DTS could be proposed as a problem-solving technique in the diagnosis of those suspected pulmonary lesions identified at the preliminary assessment of CXR.

Pairing low-dose DTS with conventional CXR eliminates the need for CT to confirm suspected lung lesions previously identified by CXR. In our series, DTS had a dramatic effect on the CT utilisation and resolved doubtful CXR findings for 256/339 (76 %) patients, reducing the need for CT to only 24 % (83/339) of patients. Once a chest opacity is suspected as being a solid pulmonary lesion by DTS, it should then go to CT for further evaluation, classification, and staging. Lower CT utilisation translated into less radiation exposure for patients. According to these results, DTS may be considered a first-line problem-solving imaging technique to rule out pulmonary lesions. Low-radiation-dose chest CT [23] could represent an alternative imaging modality, even though it appears more suitable for lung cancer screening [23, 24], while the advantage of DTS is the verification of doubtful findings directly in the X-ray unit without moving the patient to CT and with comparable effective dose to CXR and low-radiation-dose CT. The preliminary assessment of the CXR by a radiologist does

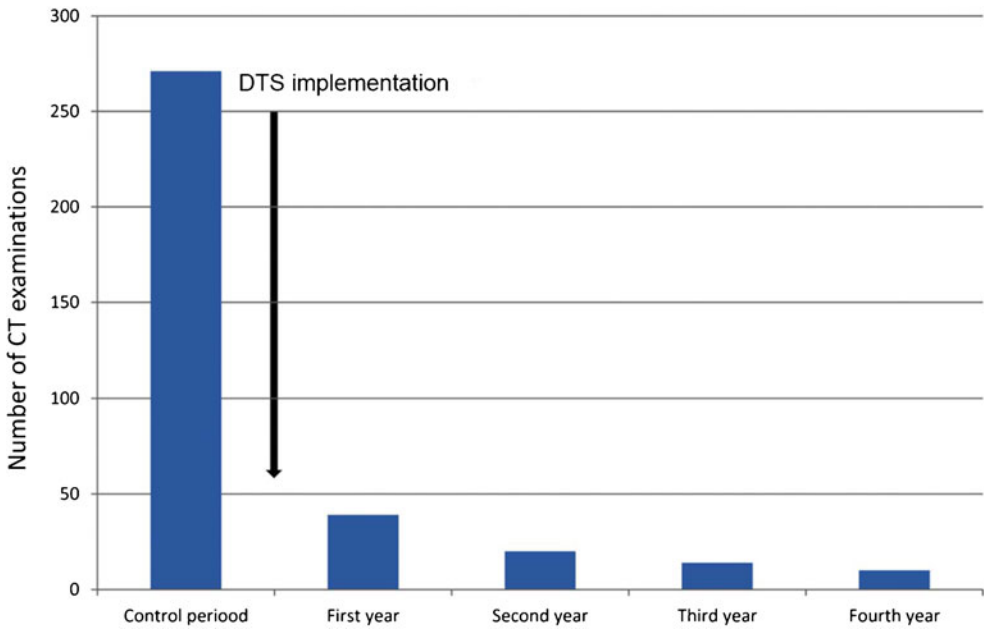

Fig. 6 Diagram shows the reduction of the number of CT examinations for suspicious chest radiography findings before and after digital tomosynthesis (DTS) implementation in our radiological department. Data collected in a 12-month control period—before DTS implementation and 1–4 years after DTS implementation

not introduce a time delay since DTS can be scheduled immediately after CXR (e.g. the same day or few days after CXR), since the examination time is comparable to CXR.

According to our results, a clear decrease in the number of CXRs considered for CT was observed after digital tomosynthesis implementation, more CTs were acquired in comparison to the following years because of the progressive decrease in the number of outpatients referred to our hospital and a corresponding increase in internal patients who presented a more advanced disease status, which was frequently related to unequivocal pulmonary lesions. Compared to CT, the main limitation of DTS is the limited depth resolution caused by the limited tomographic sweep angle. Indeed, the resolution of DTS along the *z*-axis for chest may be approximated to 2 mm [25]. In our series, all findings misinterpreted at DTS were subpleural or located in the region of the lung in the proximity of the chest wall, where the limited depth resolution of DTS may hamper the correct spatial location of the findings. This limitation is related to the geometric frontal plane acquisition by DTS, since acquisition in the sagittal plane is not recommended because of the higher dose exposure [7, 8, 26].

DTS is a fast imaging technique that offers a clear improvement in diagnostic accuracy and confidence over CXR, with a much lower radiation dose than CT. For the radiologist, DTS studies took longer to read than CXR principally because of multiple image scrolling, but the overall interpretation time was lower than CT because of the lower number of images evaluated. Even though DTS increased the interpretation time, it could be easily introduced in the routine diagnostic workflow as a case-solving technique in those patients with suspected or equivocal pulmonary lesions on CXR.

The principal limitation of our study was the inclusion of a heterogeneous group of patients who underwent CXR for different clinical reasons. The inclusion of a more selected patient cohort, e.g. patients with suspected pulmonary nodules or patients with a known primary tumour and suspected lung metastases, could provide further insights into the diagnostic accuracy of DTS. A second limitation is the absence of blinded evaluation of CXR and DTS images, since this prospective study was part of routine medical care. The third limitation is the presence of multiple reference standards including CXR for pseudolesions or overt benign lesions, and CT or histology for positive pulmonary lesions. This arose because we decided to spare patients with minor equivocal findings unnecessary CT, as usually happens in routine clinical practice.

In conclusion, DTS avoided the need for chest CT in about three-quarters of patients with suspected pulmonary lesions on CXR with a slight increase in the interpretation time and effective dose compared to CXR.

Acknowledgments We thank Dr John Sabol, GE Healthcare, for invaluable help in the VolumeRad dose calculations.

References

1. Wu N, Gamsu G, Czum J et al (2006) Detection of small pulmonary nodules using direct digital radiography and picture archiving and communication systems. J Thorac Imaging 21:27–31
2. Bley TA, Baumann T, Saueressig U et al (2008) Comparison of radiologist and CAD performance in the detection of CT-confirmed subtle pulmonary nodules on digital chest radiographs. Investig Radiol 43:343–348
3. Remy-Jardin M, Remy J, Giraud F, Marquette CH (1993) Pulmonary nodules: detection with thick-section spiral CT versus conventional CT. Radiology 187:513–520
4. Rubin GD, Lyo JK, Paik DS et al (2005) Pulmonary nodules on multi-detector row CT scans: performance comparison of radiologists and computer-aided detection. Radiology 234:274–283
5. Dobbins JT III, Godfrey DJ (2003) Digital x-ray tomosynthesis: current state of the art and clinical potential. Phys Med Biol 48: R65–R106
6. Dobbins JT, Mc Adams HP, Devon G, Li CM (2008) Digital tomosynthesis of the chest. J Thorac Imaging 23:86–92
7. Dobbins JT, Mc Adams HP, Song JW et al (2008) Digital tomosynthesis of the chest for lung nodule detection: interim sensitivity results from an ongoing NIH-sponsored trial. Med Phys 35:2554–2557
8. Vikgren J, Zachrisson S, Svalkvist A et al (2008) Comparison of chest tomosynthesis and chest radiography for detection of pulmonary nodules: human observer study of clinical cases. Radiology 249:1034–1041
9. Gomi T, Nakajima M, Fujiwara H, Umeda T (2011) Comparison of chest dual-energy subtraction digital tomosynthesis imaging and dual-energy subtraction radiography to detect simulated pulmonary nodules with and without calcifications a phantom study. Acad Radiol 18:191–196
10. Yamada Y, Jinzaki M, Hasegawa I et al (2011) Fast scanning tomosynthesis for the detection of pulmonary nodules: diagnostic performance compared with chest radiography using multidetector-row computed tomography as the reference. Investig Radiol 46:471–477
11. Quaia E, Baratella E, Cioffi V, Bregant P, Cernic S, Cuttin R, Cova MA (2010) The value of digital tomosynthesis in the diagnosis of suspected pulmonary lesions on chest radiography: analysis of diagnostic accuracy and confidence. Acad Radiol 17:1267–1274
12. Kim EY, Chung MJ, Lee HY, Koh WJ, Jung HN, Lee KS (2010) Pulmonary mycobacterial disease: diagnostic performance of low-dose digital tomosynthesis as compared with chest radiography. Radiology 257:269–277
13. Hansell DM, Bankier A, Mac Mahon H, McLoud T, Muller NL, Remy J (2008) Fleischner society: glossary of terms for thoracic imaging. Radiology 246:697–722
14. Servomaa A, Tapiovaara M (1998) Organ dose calculation in medical X ray examinations by the program PCXMC. Radiat Prot Dosim 80:213–219
15. Cristy M, Eckerman KR (1987) Specific absorbed fractions of energy at various ages from internal photon sources. I. Method. Publication no. ORNL/TM-8381, Oak Ridge National Laboratory, Oak Ridge (USA)
16. Sabol JM (2009) A Monte Carlo estimation of effective dose in chest tomosynthesis. Med Phys 36:5480–5487
17. European Guidelines on Quality Criteria for Computed Tomography (1999) Report EUR 16262. European Commission, Brussels. Available at: http://www.drs.dk/guidelines/ct/quality/index.htm

18. Campbell MJ, Machin D (1999) Medical statistics, a commonsense approach. Wiley, Chichester, pp 85–89
19. Beck JR, Shultz EK (1986) The use of relative operating characteristic (ROC) curves in test performance evaluation. Arch Pathol Lab Med 110:13–20
20. Hanley JA, McNeil BJ (1983) A method of comparing the areas under receiver operating characteristic curves derived from the same cases. Radiology 148:839–843
21. Kundel HL, Polansky M (2003) Measurement of observer agreement. Radiology 228:303–308
22. Erasmus JJ, Connolly JE, McAdams HP, Roggli VL (2000) Solitary pulmonary nodules. I. Morphologic evaluation for differentiation of benign and malignant lesions. RadioGraphics 20:43–58
23. Zhu X, Yu J, Huang Z (2004) Low-dose chest CT: optimizing radiation protection for patients. AJR Am J Roentgenol 183:809–816
24. Gierada DS, Pilgram TK, Ford M et al (2008) Lung cancer: interobserver agreement on interpretation of pulmonary findings at low-dose CT screening. Radiology 246:265–272
25. Li B, Avinash GB (2007) Optimization of slice sensitivity profile for radiographic tomosynthesis. Med Phys 34:2907–2916
26. Godfrey DJ, McAdams HP, Dobbins JT (2006) Optimization of the matrix inversion tomosynthesis (MITS) impulse response and modulation transfer function characteristics for chest imaging. Med Phys 33:655–667